New Measurements of the Beam Normal Spin Asymmetries at Large Backward Angles with Hydrogen and Deuterium Targets

D. Balaguer Ríos,[1,†] K. Aulenbacher,[1] S. Baunack,[1] J. Diefenbach,[1] B. Gläser,[1] D. von Harrach,[1] Y. Imai,[1] E.-M. Kabuß,[1] R. Kothe,[1] J. H. Lee,[1] H. Merkel,[1] M. C. Mora Espí,[1] U. Müller,[1] E. Schilling,[1] C. Weinrich,[1] L. Capozza,[1,2] F. E. Maas,[1,2] J. Arvieux,[3,*] M. A. El-Yakoubi,[3] R. Frascaria,[3] R. Kunne,[3] M. Morlet,[3] S. Ong,[3] J. van de Wiele,[3] S. Kowalski,[4] and Y. Prok[4]

[1]*Institut für Kernphysik, Johannes Gutenberg-Universität Mainz, J.J. Becherweg 45, D-55099 Mainz, Germany*
[2]*Helmholtz-Institut Mainz, Johannes Gutenberg-Universität Mainz, J.J. Becherweg 36, D-55099 Mainz, Germany*
[3]*Institut de Physique Nucléaire, CNRS-IN2P3, Université Paris-Sud, F-91406 Orsay Cedex, France*
[4]*Laboratory for Nuclear Science and Department of Physics, MIT, Cambridge, Massachusetts 02139, USA*

(Received 14 December 2016; revised manuscript received 5 May 2017; published 6 July 2017)

New measurements of the beam normal single spin asymmetry in the electron elastic and quasielastic scattering on the proton and deuteron, respectively, at large backward angles and at $\langle Q^2 \rangle = 0.22$ $(\mathrm{GeV}/c)^2$ and $\langle Q^2 \rangle = 0.35$ $(\mathrm{GeV}/c)^2$ are reported. The experimentally observed asymmetries are compared with the theoretical calculation of Pasquini and Vanderhaeghen [Phys. Rev. C **70**, 045206 (2004).]. The agreement of the measurements with the theoretical calculations shows a dominance of the inelastic intermediate excited states of the nucleon, πN and the Δ resonance. The measurements explore a new, important parameter region of the exchanged virtual photon virtualities.

DOI: 10.1103/PhysRevLett.119.012501

The exchange of two hard virtual photons in the elastic electron-nucleon scattering beyond the one-photon exchange Born approximation has been the subject of recent investigation [1,2]. Two complementary methods, a determination from a measurement of a differential cross section using unpolarized electrons (Rosenbluth separation) and the measurement of the polarization transfer to the proton final state, gave significantly different results for $\mu_p G_E^p / G_M^p$. The two-photon exchange has been addressed as the explanation for such a discrepancy. Other observables in which the two-photon exchange physics plays a role are: neutron form factors, resonance electroproduction, the pion form factor and the elastic electron-nucleus cross section, in particular deuteron and ^{3}He [1]. The exchange of two virtual photons implies the excitation of nucleon intermediate states offering the possibility of testing models of hadronic structure [3–22]. In contrast to previous measurements at forward [23,24] and close to right angles [25], the A4 measurements presented in this work have been performed at large backward angles. The A4 measurements explore a new important parameter region of the virtualities of the exchanged virtual photons, involved in the theoretical calculation of the nucleon intermediate states, see Fig. 2 from Ref. [11]. Moreover, in contrast to the SAMPLE measurement [26], at similar backward scattering angle, the A4 measurements have improved the precision by a factor ∼4. The A4 measurements have been performed at larger beam energies, probing the πN and Δ resonance inelastic intermediate states.

The two-photon exchange physics affects the parity violating asymmetry through the normalization to the electromagnetic amplitude [27] and it is of special relevance in precision measurements of the weak charge of the proton at low Q^2 like Q_{weak} [28] and $P2$ [29]. It is also useful in the theoretical determination of the γZ box diagrams which also takes part in the proton weak charge radiative corrections [30–33].

Two-photon exchange effects can be observed in radiative corrections to the cross section, the ratio in $e^- p$ and $e^+ p$ elastic scattering cross sections, the depolarization tensor, and the target and beam normal single spin asymmetries [34–37]. Six generalized form factors depending on two kinematic variables parametrize the elastic electron-proton scattering $\tilde{G}_M(s, Q^2)$, $\tilde{G}_E(s, Q^2)$, and $\tilde{F}_i(\nu, Q^2)$; $i = 3, \ldots, 6$ [34,38]. These form factors reduce to $G_M(Q^2)$, $G_E(Q^2)$ in the Born approximation. The spin averaged elastic cross section depends on $|\tilde{G}_E|$, $|\tilde{G}_M|$, and $\mathrm{Re}\tilde{F}_3$. Its calculation involves the off-shell form factors of the nucleon and the off-shell transition form factors of the intermediate excited states. There is a calculation of the cross section, assuming only the on-shell ground intermediate state of the nucleon, which is able to partially solve the mentioned discrepancy in the extraction of $\mu_p G_E^p / G_M^p$ [10]. There are also partonic calculations which resort to generalized parton distributions of the nucleon and are able to resolve the discrepancy at large Q^2 [12,16].

The T-odd observables target and beam normal spin asymmetries arise from the interference of the one-photon and two-photon exchange amplitudes, see Fig. 1 in Ref. [39]. The target normal spin asymmetry depends on the imaginary part of $\tilde{G}_E$, $\tilde{G}_M$, and $\tilde{F}_3$ while the beam

normal spin asymmetry depends on the imaginary part of $\tilde{F}_3$, $\tilde{F}_4$, and $\tilde{F}_5$ [11,40]. These asymmetries are zero in the Born approximation. They are proportional to the fine structure constant α. For the beam normal spin asymmetry $A_\perp$ there is an additional suppression of the electron polarization by a factor $1/\gamma$. It would be zero in the limit of massless electrons. $A_\perp$ is therefore of the order 10^{-5} for a beam energy less than 1 GeV. The measurement of $A_\perp$ is so far the only measured observable to access the imaginary part of $\tilde{F}_4$ and $\tilde{F}_5$. Moreover, it allows for a test of models of the excitation of the intermediate state in the double virtual Compton scattering on the nucleon.

The first measurement of the SAMPLE experiment of $A_\perp$ in the elastic electron-proton scattering is at backward angles at $Q^2 = 0.1$ $(\mathrm{GeV}/c)^2$ [26]. There are more recent measurements of the A4 experiment at forward angles at $Q^2 = 0.11, 0.23$ $(\mathrm{GeV}/c)^2$ [39] with hydrogen, the G0 experiment at $Q^2 = 0.15, 0.25$ $(\mathrm{GeV}/c)^2$ at forward angles angles with hydrogen [23], and at $Q^2 = 0.22, 0.63$ $(\mathrm{GeV}/c)^2$ at backward angles with hydrogen and deuterium [25], the measurements of Happex at GeV energies, which include besides the hydrogen target heavier nuclei [24], and the preliminary measurements of the Q_{weak} experiment in the elastic electron-proton scattering and in the inelastic scattering on hydrogen, aluminum, and carbon [41]. There is a very recent measurement of the A1 experiment at MAMI of $A_\perp$ in the reaction $^{12}\mathrm{C}(\vec{e}, e')^{12}\mathrm{C}$ [42,43]. In this Letter we present the measurements of the A4 experiment at backward angles $\langle\theta\rangle = 145°$ and beam energies $E = 315$ and 420 MeV, corresponding to $Q^2 = 0.22$ and 0.35 $(\mathrm{GeV}/c)^2$, respectively, with both hydrogen and deuterium targets.

The beam normal spin asymmetry is defined as $A_\perp = (\sigma^\uparrow - \sigma^\downarrow/\sigma^\uparrow + \sigma^\downarrow)$, where $\sigma^{\uparrow(\downarrow)}$ refers to the cross section with the spin of the electron parallel (antiparallel) to the vector $\vec{S} = (\vec{k} \times \vec{k}'/|\vec{k} \times \vec{k}'|)$ in the direction perpendicular to the scattering plane.

In the experimental configuration the polarization vector $\vec{P}$ is perpendicular to the beam direction and it is contained in the horizontal plane, see Fig. 2 in Ref. [39]. $A_\perp$ reaches a maximum when the scattering plane is perpendicular to $\vec{P}$ $(\varphi = \pi/2)$ and it is zero when the scattering plane contains $\vec{P}(\varphi = 0)$. $A_\perp$ is azimuthally modulated, see Fig. 1:

$$A_\perp = A_{\perp,0}\vec{P} \cdot \frac{\vec{k} \times \vec{k}'}{|\vec{k} \times \vec{k}'|} = -A_{\perp,0} \cos\varphi. \qquad (1)$$

The cosine modulation on the azimuthal angle and the minus sign are determined by the coordinate system of the detector and the direction of the polarization of the electron beam, see Fig. 2 in Ref. [39].

The A4 experiment [39,44–53] at the MAMI microtron facility uses a transversely polarized electron beam of 20 μA to measure $A_\perp$. Details of the experimental setup can be found in Ref. [39]. The electron beam source

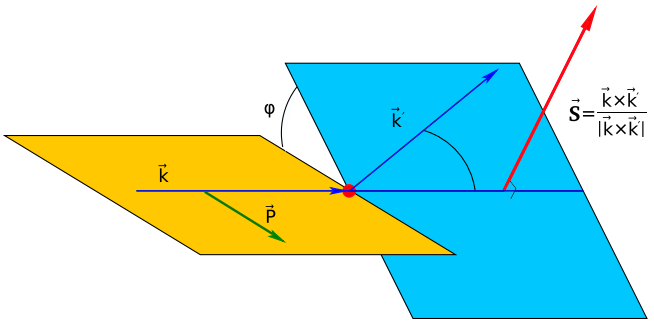

FIG. 1. The polarization vector $\vec{P}$ of the electron is perpendicular to the momentum of the incoming electron beam $\vec{k}$ and it is contained in the horizontal plane. $\vec{k}'$ is the momentum of the scattered electron and $\vec{S}$ is the vector normal to the scattering plane. $A_\perp$ is modulated by the azimuthal angle φ by the projection $\vec{P} \cdot \vec{S}$

generates longitudinally polarized electrons from a superlattice photocathode illuminated by a circularly polarized laser beam. A Mott and a Mø ller polarimeter are used once a week to measure the polarization of about 80%. The spin direction is adjusted using a Wien Filter. The spin direction is flipped using a Pockel cell with a frequency of 50 Hz. The spin flip is produced randomly according to the patterns $+--+$ and $-++-$. A $\lambda/2$ wave plate is inserted and removed every week of data taking, in order to suppress systematic effects and to check the correct change of sign of the experimentally observed asymmetry.

The target cell contains liquid H_2 or D_2. The length of the target cell is 23.3 cm. The luminosity amounts to 1.23×10^{-38} $\mathrm{cm}^{-2}\,\mathrm{s}^{-1}$ and 1.41×10^{-38} $\mathrm{cm}^{-2}\,\mathrm{s}^{-1}$ for the H_2 and the D_2 target, respectively. The detector consists of a segmented, totally absorbing electromagnetic calorimeter of 1022 PbF_2 crystals arranged in 146 slices and 7 rings. It possesses axial symmetry covering a 2π azimuthal angle. The energy resolution allows us to separate elastically from inelastically scattered electrons. It covers the polar angle interval $[140°, 150°]$ in the backward angles configuration. In front of the calorimeter 72 plastic scintillators are installed to discriminate neutral and charged particles. At backward angles the energy of the scattered electrons is smaller than at forward angles so that the (quasi)elastic peak is hidden by the background of neutral particles. The detector has a dead time of 20 ns. The events are registered by fast electronics and four histograms are generated: the energy spectra of neutral and charged particles for each polarization state.

The number of counts for each polarization state are obtained integrating under the elastic and quasielastic peak, for the H_2 and D_2 target, respectively, between a lower cut value and an upper cut value. The asymmetry in the number of counts $(N^\uparrow - N^\downarrow/N^\uparrow + N^\downarrow)$ is extracted from each module (crystal) for every run of five minutes from the spectrum of charged particles. The amount of the neutral

background and its asymmetry have been determined from the measured spectrum of neutral particles with high precision. The method for the neutral background correction has been described in detail in Refs. [51,53].

The extracted asymmetries are cross section weighted averaged over the five inner rings (polar angle). Then they are averaged over the whole sample of five-minute runs for each $\lambda/2$-wave plate data set. And finally, they are error weighted and averaged for each $\lambda/2$-wave plate data set, changing the sign of the asymmetry for the "in" sets. The result is $A_{\perp,i}$ as a function of the slice (azimuthal angle φ).

$A_{\perp,i}$ exhibits the expected sinusoidal modulation, see Fig. 2. The function $-A\cos(\varphi+\delta)+p$ is fitted to the sample of $A_{\perp,i}$. The phase δ and the offset p yield values compatible with zero. The final value of the asymmetry is obtained averaging the amplitude of the asymmetry for each slice $\langle A_{\perp,0}\rangle = \langle A_{\perp,i}/\cos\varphi_i\rangle$. The average over the cosine modulation increases the errors by a factor $\sim\sqrt{2}$.

The asymmetry has also been corrected from the background of quasielastic scattering in the nuclei of the aluminum windows, whose asymmetry has been calculated from the theoretical $A_\perp^p$ and $A_\perp^n$, assuming the static approximation [11,14,54] and from the background of random coincidence events, whose amount and asymmetry are estimated from the spectrum of neutral particles. There is a background from the elastic scattering on the deuteron for the deuterium data. Its amount is 0.3% and 0.1% for the beam energies 315 MeV and 420 MeV, respectively. Its effect has been neglected. $A_\perp$ has also been corrected for the false asymmetry from helicity correlated differences in the energy, position, angle, and current of the electron beam as well as for the target density fluctuations. Table I shows an example of the budget of systematic corrections and errors for the data with H_2 target and energy 315 MeV.

As a systematic test it is verified that $A_\perp$ changes sign for the samples, where the $\lambda/2$ wave plate has been inserted.

The measured $A_\perp$ at the mean angle $\langle\theta\rangle = 145°$ for the hydrogen target and deuterium are as follows.

At the beam energy 315 MeV, corresponding to $\langle Q^2\rangle = 0.22\ (\mathrm{GeV}/c)^2$:

$$A_\perp^p = (-94.83 \pm 6.02_{\mathrm{stat}} \pm 4.07_{\mathrm{sys}}) \times 10^{-6}$$
$$A_\perp^d = (-56.42 \pm 4.53_{\mathrm{stat}} \pm 2.84_{\mathrm{sys}}) \times 10^{-6}.$$

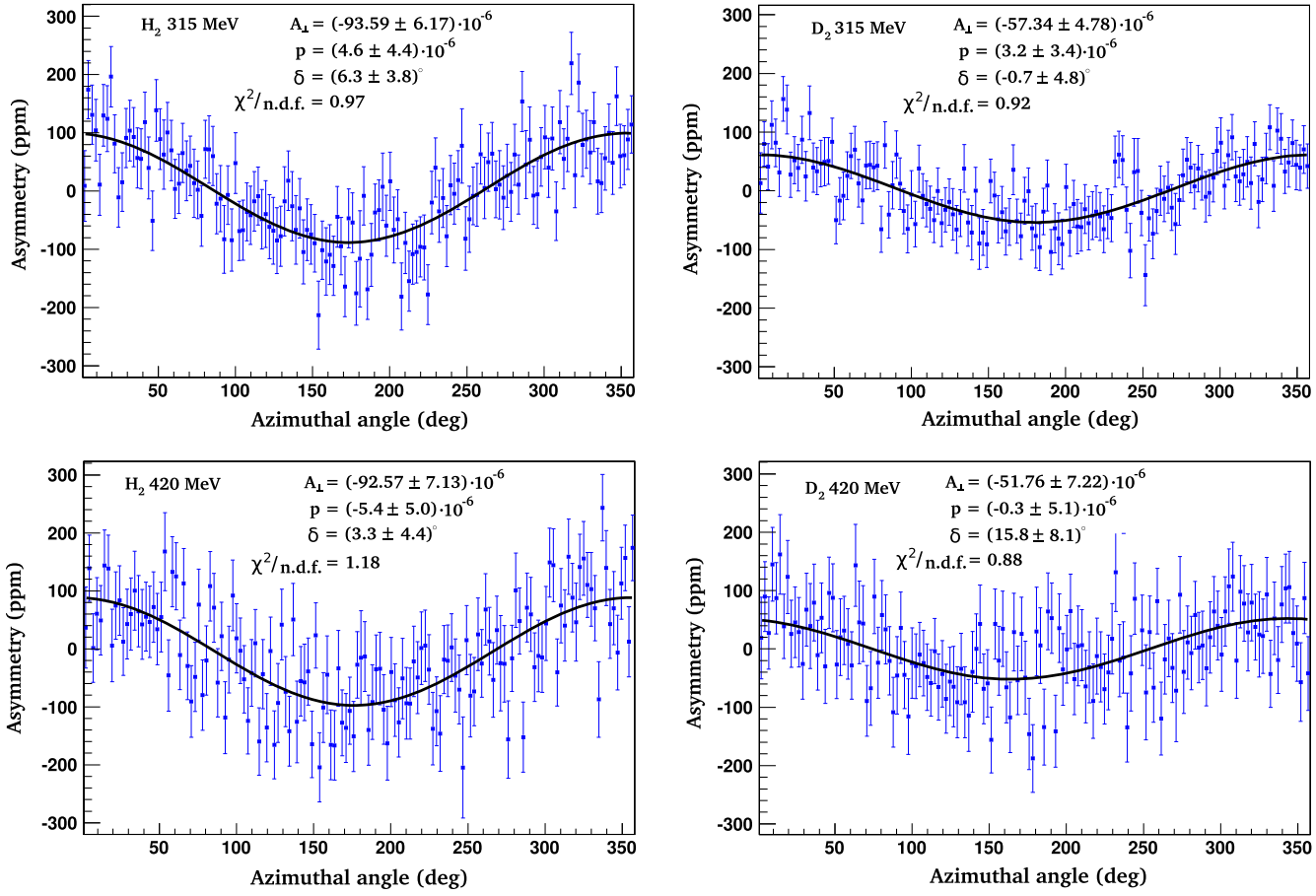

FIG. 2. The figures show the extracted beam normal spin asymmetries for H_2 and D_2 target and beam energies 315 MeV and 420 MeV as a function of the azimuthal angle φ. The function $-A_\perp\cos(\varphi+\delta)+p$ with a phase δ and an offset p is fitted to the data. The phase and offset of the fits are in all cases compatible with zero, demonstrating the cosine dependence of the asymmetry on φ.

TABLE I. Systematic corrections to the asymmetry and their contribution to the systematic uncertainty for the data corresponding to the H_2 target and energy 315 MeV.

	Scaling factor	Error (ppm)
Polarization	0.77	3.72
	Correction (ppm)	Error (ppm)
Dilution of γ background	−4.00	1.54
Helicity correlated beam differences	0.00	0.00
Al windows	−1.96	0.51
Random coincidence events	−0.82	0.15
Target density	1.06	0.20
Spin angle deviation	−0.07	0.13
Sum systematic errors	4.07	

At the beam energy 420 MeV, corresponding to $\langle Q^2 \rangle = 0.35\ (\mathrm{GeV}/c)^2$:

$$A_\perp^p = (-99.55 \pm 6.73_{\mathrm{stat}} \pm 4.63_{\mathrm{sys}}) \times 10^{-6}$$
$$A_\perp^d = (-53.40 \pm 6.95_{\mathrm{stat}} \pm 2.98_{\mathrm{sys}}) \times 10^{-6}.$$

Figure 3 shows the comparison of the measurements with the theoretical expectations [11,54]. The theoretical calculation involves the absorptive part of the doubly virtual Compton scattering tensor of the nucleon. The intermediate state has been calculated using the phenomenological pion electroproduction amplitudes $\gamma^* N \to X$, where $X = \pi N, \Delta$, using the isobar model MAID [55]. The theoretical calculation has been done for the proton and neutron. We have combined the calculations of $A_\perp^p$ and $A_\perp^n$ assuming the static approximation, with a cross section weighted average, to compare directly with the experimentally observed $A_\perp^d$. The calculated $A_\perp^p$ and $A_\perp^n$ exhibit opposite sign since at backward angles the asymmetry is approximately proportional to the nucleon magnetic magnetic moment [11]. The agreement of the theoretical calculation $A_\perp^p$ with the measurement confirms the predominance of the inelastic intermediate states of the nucleon, which include the πN and the Δ resonance intermediate states. The calculation for the deuteron is slightly smaller than the measurements. Since the calculation for the proton agrees with the measurements, it is reasonable to expect that the calculation for the neutron is also valid. Under this assumption, the small deviation of the deuteron calculation and the deuteron measurements could be interpreted as a hint of the reliability of the static approximation. The measured $A_\perp^p$ by SAMPLE [26] at a beam energy 200 MeV is larger (more negative) than the theoretical calculation. At this energy the elastic and inelatic contribution are of opposite sign and the inelastic contribution is small, since it incorporates only intermediate states at the pion production threshold [11]. At beam energies of 315 MeV and 420 MeV, the A4 measured asymmetries are much larger. At these beam energies the elastic contribution is negligible and the magnitude of the asymmetry is driven by the inelastic intermediate states [11].

In conclusion the A4 measurements of $A_\perp$ at backward angles demonstrate the reliability of the theoretical calculations of Pasquini *et al.* [11]. They are the first at large backward angles and at high beam energies and Q^2, allowing access to πN and to the Δ resonance intermediate

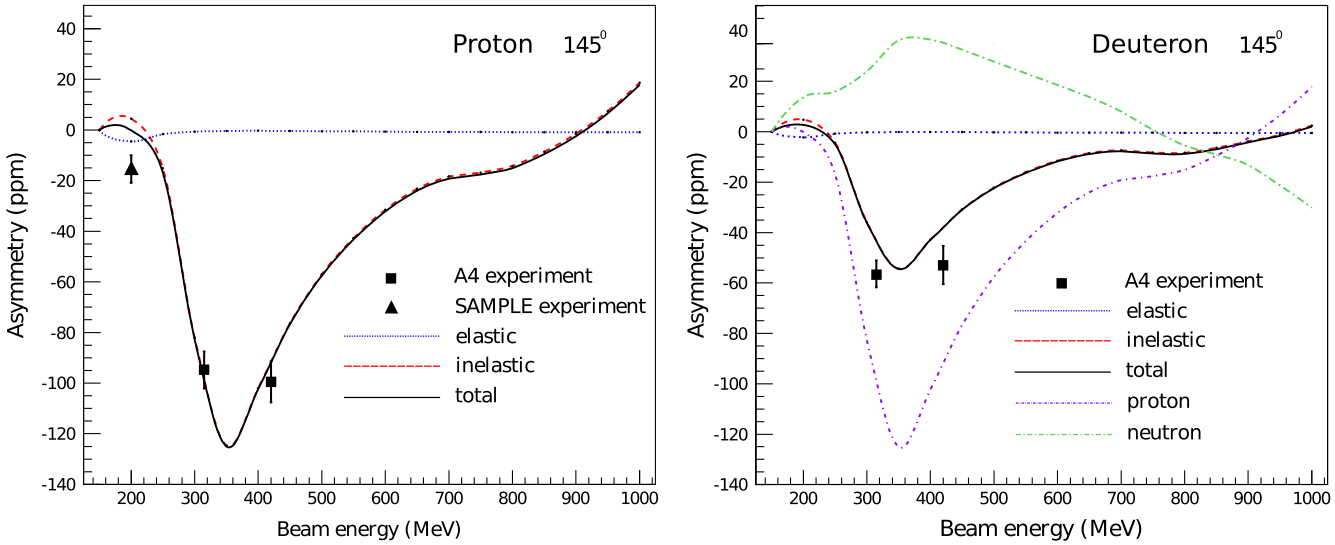

FIG. 3. The figures show the comparison of the measured $A_\perp$ by the A4 and SAMPLE experiments on the proton and the deuteron with the theoretical calculations of Pasquini *et al.* The dotted line represents the contribution to $A_\perp$ of the ground state of the nucleon (elastic). The dashed line corresponds to the excited intermediate states (inelastic). The solid line is the sum of both contributions. The figure on the left corresponds to a proton target and the one on the right to a deuteron target, where the static approximation has been used to calculate the asymmetries on the deuteron from those ones on the proton and neutron.

states and extending the parameter region of the exchanged photon virtualities, see Fig. 2 from Ref. [11]. Further measurements of the A4 experiment at forward angles and different Q^2 are under analysis and will provide more data for the comparison at different kinematics.

This work has been supported by the Deutsche Forschungsgemeinschaft (DFG) within the projects SFB 443, SFB 1044, and the PRISMA excellence cluster. We would like to thank the crew of the MAMI accelerator for the high beam quality.

*Deceased.
†dabarios@kph.uni-mainz.de

[1] J. Arrington, P. G. Blunden, and W. Melnitchouk, Prog. Nucl. Part. Phys. **66**, 782 (2011).
[2] C. E. Carlson, and M. Vanderhaeghen, Annu. Rev. Nucl. Part. Sci. **57**, 171 (2007).
[3] S. D. Drell and M. Ruderman, Phys. Rev. **106**, 561 (1957).
[4] S. D. Drell and S. Fubini, Phys. Rev. **113**, 741 (1959).
[5] N. R. Werthammer and M. A. Ruderman, Phys. Rev. **123**, 1005 (1961).
[6] J. A. Campbell, Nucl. Phys. **B1**, 283 (1967).
[7] J. A. Campbell, Phys. Rev. **180**, 1541 (1969).
[8] J. A. Campbell, Phys. Rev. **184**, 1860 (1969).
[9] R. W. Brown *et al.*, Phys. Rev. D **1**, 1432 (1970).
[10] P. G. Blunden, W. Melnitchouk, and J. A. Tjon, Phys. Rev. Lett. **91**, 142304 (2003).
[11] B. Pasquini, and M. Vanderhaeghen, Phys. Rev. C **70**, 045206 (2004).
[12] Y. C. Chen, A. Afanasev, S. J. Brodsky, C. E. Carlson, and M. Vanderhaeghen, Phys. Rev. Lett. **93**, 122301 (2004).
[13] M. Gorchtein, P. A. M Guichon, and M. Vanderhaeghen, Nucl. Phys. **A741**, 234 (2004).
[14] B. Pasquini, and M. Vanderhaeghen, Eur. Phys. J. A **24**, 29 (2005).
[15] P. G. Blunden, W. Melnitchouk, and J. A. Tjon, Phys. Rev. C **72**, 034612 (2005).
[16] A. V. Afanasev *et al.*, Phys. Rev. Lett. **72**, 013008 (2005).
[17] S. Kondratyuk, P. G. Blunden, W. Melnitchouk, and J. A. Tjon, Phys. Rev. Lett. **95**, 172503 (2005).
[18] M. Gorchtein, Phys. Lett. B **644**, 322 (2007).
[19] C. E. Carlson, and M. Vanderhaeghen, Annu. Rev. Nucl. Part. Sci. **57**, 171 (2007).
[20] S. Kondratyuk, and P. G. Blunden, Phys. Rev. C **75**, 038201 (2007).
[21] N. Kivel, and M. Vanderhaeghen, Phys. Rev. Lett. **103**, 092004 (2009).
[22] D. Borisyuk, and A. Kobushkin, Phys. Rev. D **79**, 034001 (2009).
[23] D. S. Armstrong *et al.* (G0 Collaboration), Phys. Rev. Lett. **99**, 092301 (2007).
[24] S. Abrahamyan *et al.* (HAPPEX and PREX Collaborations), Phys. Rev. Lett. **109**, 192501 (2012).
[25] D. Androić *et al.* (G0 Collaboration), Phys. Rev. Lett. **107**, 022501 (2011).
[26] S. Wells *et al.*, Phys. Rev. C **63**, 064001 (2001).
[27] J. A. Tjon, and W. Melnitchouk, Phys. Rev. Lett. **100**, 082003 (2008).
[28] D. Androić *et al.* (Q_{weak} Collaboration), Phys. Rev. Lett. **111**, 141803 (2013).
[29] D. Becker, K. Gerz, S. Baunack, K. S. Kumar, and F. E. Maas (*P*2 Collaboration), AIP Conf. Proc. **1563**, 78 (2013).
[30] M. Gorchtein, and C. J. Horowitz, Phys. Rev. Lett. **102**, 091806 (2009).
[31] M. Gorchtein, C. J. Horowitz, M. J. Ramsey-Musolf, R. Alarcon, P. Cole, A. J. Kreiner, and H. F. Arellano, AIP Conf. Proc. **1265**, 328 (2010).
[32] A. Sibirtsev, P. G. Blunden, W. Melnitchouk, and A. W. Thomas, Phys. Rev. D **82**, 013011 (2010).
[33] B. C. Rislow and C. E. Carlson, Phys. Rev. D **83**, 113007 (2011).
[34] M. P. Rekalo, and E Tomasi-Gustafsson, Nucl. Phys. **740**, 271 (2004).
[35] I. A. Rachek *et al.*, Phys. Rev. Lett. **114**, 062005 (2015).
[36] D. Rimal *et al.* (CLAS Collaboration), Phys. Rev. C **95**, 065201 (2017).
[37] B. S. Henderson *et al.* (OLYMPUS), Phys. Rev. Lett. **118**, 092501 (2017).
[38] M. L. Goldberger, Y. Nambu, and R. Oehme, Ann. Phys. (N.Y.) **2**, 226 (1957).
[39] F. E. Maas *et al.*, Phys. Rev. Lett. **94**, 082001 (2005).
[40] A. De Rújula, J. M. Kaplan, and E. de Rafael, Nucl. Phys. **B35**, 365 (1971).
[41] B. P. Waidyawansa *et al.* (Q_{weak} Collaboration), arXiv: 1604.04602.
[42] M. Thiel *et al.*, *Proc. Sci. (Bormio 2015)* 025 (2015).
[43] A. Esser *et al.*, *Proc. Sci. (Bormio 2016)* 026 (2016).
[44] S. Köbis *et al.*, Nucl. Phys. **B61**, 625 (1998).
[45] P. Achenbach *et al.* (A4), Nucl. Instrum. Methods Phys. Res., Sect. A **416**, 357 (1998).
[46] P. Achenbach, S. Baunack, K. Grimm, T. Hammel, D. von Harrach, A.Lopes Ginja, F. E. Maas, E. Schilling, and H. Ströher (A4), Nucl. Instrum. Methods Phys. Res., Sect. A **465**, 318 (2001).
[47] F. E. Maas *et al.* (A4), Phys. Rev. Lett. **93**, 022002 (2004).
[48] F. E. Maas *et al.* (A4), Phys. Rev. Lett. **94**, 152001 (2005).
[49] T. Hammel *et al.* (A4), Nucl. Instrum. Methods Phys. Res., Sect. A **564**, 1 (2006).
[50] I. Altarev *et al.* (A4), Nucl. Instrum. Methods Phys. Res., Sect. A **564**, 13 (2006).
[51] S. Baunack *et al.* (A4), Phys. Rev. Lett. **102**, 151803 (2009).
[52] S. Baunack *et al.* (A4), Nucl. Instrum. Methods Phys. Res., Sect. A **640**, 58 (2011).
[53] D. Balaguer *et al.* (A4), Phys. Rev. D **94**, 051101 (2016).
[54] B. Pasquini (private communication).
[55] L. Tiator, D. Drechsel, O. Hanstein, S. S. Kamalov, and S. N. Yang, Nucl. Phys. **A689**, 205 (2001).